Carbohydrate Polymers 83 (2011) 483–488

Contents lists available at ScienceDirect

Carbohydrate Polymers

journal homepage: www.elsevier.com/locate/carbpol

Crystal transition from Na–cellulose IV to cellulose II monitored using synchrotron X-ray diffraction

Kayoko Kobayashi [a], Satoshi Kimura [a], Eiji Togawa [b], Masahisa Wada [a,c,*]

[a] Department of Biomaterials Science, Graduate School of Agricultural and Life Sciences, The University of Tokyo, Tokyo 113-8657, Japan
[b] Forestry and Forest Products Research Institute, Matsunosato 1, Tsukuba, Ibaraki 305-8687, Japan
[c] Department of Plant & Environmental New Resources, College of Life Sciences, Kyung Hee University, 1, Seocheon-dong, Giheung-ku, Yongin-si, Gyeonggi-do 446-701, Republic of Korea

ARTICLE INFO

Article history:
Received 29 June 2010
Received in revised form 30 July 2010
Accepted 5 August 2010
Available online 11 August 2010

Keywords:
Na–cellulose IV
Cellulose II
Mercerization
Synchrotron X-ray fiber diffraction
Solid-state ^{13}C NMR
Crystal transition

ABSTRACT

Oriented samples of Na–cellulose IV, a hydrate form of cellulose II, were prepared from ramie fibers by mercerization. Crystal transition from Na–cellulose IV to cellulose II was monitored using synchrotron X-ray fiber diffraction under a controlled relative humidity. During drying of the Na–cellulose IV, the *d*-spacing of the $(1\,\bar{1}\,0)$ plane gradually decreased while the *d*-spacings of the (1 1 0), (0 2 0), and (0 0 2) planes remained almost constant. From these results, the transition mechanism from Na–cellulose IV to cellulose II can be understood as crystalline lattice contraction of Na–cellulose IV along the *a*-axis direction while maintaining its hydrophobic stacking sheet structure. In addition, the lattice contraction of Na–cellulose IV on dehydration occurred continuously throughout the drying process, and no clear transition point was observed. This dehydration behavior and instability of Na–cellulose IV implies a random location of water molecules in the crystalline lattice. Following the drying process, dried cellulose II was immersed in water, but it did not return to the Na–cellulose IV form. Therefore, the transformation from Na–cellulose IV to cellulose II was irreversible.

1. Introduction

Mercerization is a simple treatment of native cellulose fibers using an alkali solution that was discovered in the nineteenth century by John Mercer (Heines, 1944). This treatment is still used in the textile industry because it gives luster and improves the mechanical properties and dyeing affinity of cellulose fibers. Carrying out mercerization using a particular concentration of alkali solutions means that the two naturally occurring crystal forms of cellulose, cellulose I_α, and cellulose I_β (collectively known as cellulose I) (Atalla & VanderHart, 1984; VanderHart & Atalla, 1984), are converted into another polymorph, cellulose II, through several intermediate alkali-celluloses (Warwiker, 1971).

These intermediate structures formed during mercerization have been studied using X-ray diffraction (Hess and Trogus, 1931; Nishimura, Okano, & Sarko, 1991; Nishimura and Sarko, 1991; Okano & Sarko, 1984, 1985; Sobue, Kiessig, & Hess, 1939; Whitaker, Nieduszynski, & Atkins, 1974) and solid-state ^{13}C NMR spectroscopy (Kamide, Kowsaka, & Okajima, 1985; Kunze, Ebert, Schröter, Frigge, & Philipp, 1981; Philipp, Kunze, & Fink, 1987; Porro, Bédué, Chanzy, & Heux, 2007; Takahashi & Ohkubo, 1993; Takahashi, Ookubo, & Takenaka, 1991; Yamada, Kowsaka, Matsui, Okajima, & Kamide, 1992; Yokota, Sei, Horii, & Kitamaru, 1990). The following transition scheme on mercerization is generally accepted as being correct. Immersion of natural cellulose fibers, such as ramie and cotton, into a 3–5N NaOH solution leads to a penetration of the alkali solution between the cellulose molecular chains, which form a complex with the alkali ions and water molecules, called Na–cellulose I. On washing Na–cellulose I with excess water, the alkali ions are excluded from the crystalline lattice, and this is converted into another intermediate form, Na–cellulose IV. Na–cellulose IV has no alkali ions in its crystalline lattice, and is the hydrate form of cellulose II. This is also supported by the fact that a simple drying of Na–cellulose IV converts it into cellulose II.

Nishimura and Sarko (1991) reported on the crystal structure of Na–cellulose IV using X-ray diffraction analysis and stereochemical modeling. The model they proposed is based on a two-chain monoclinic $P2_1$ unit cell ($a = 9.57$ Å, $b = 8.72$ Å, $c = 10.35$ Å, and $\gamma = 122.0^\circ$) that contains two water molecules with antiparallel chain packing. This unit cell is larger by about 9% from the two-chain monoclinic unit cell of mercerized cellulose II having dimensions of $a = 8.10$ Å, $b = 9.03$ Å, $c = 10.31$ Å, and $\gamma = 117.10^\circ$ (Langan, Nishiyama, & Chanzy, 2001) due to intercalated water molecules.

* Corresponding author at: Department of Biomaterials Science, Graduate School of Agricultural and Life Sciences, The University of Tokyo, Tokyo 113-8657, Japan. Tel.: +81 3 5841 5247; fax: +81 3 5841 2677.
E-mail address: awadam@mail.ecc.u-tokyo.ac.jp (M. Wada).

0144-8617/$ – see front matter © 2010 Elsevier Ltd. All rights reserved.
doi:10.1016/j.carbpol.2010.08.006

All of the water molecules located between the corner chains form hydrogen bonds with the surrounding cellulose chains.

Recently, we reported that the conversion of cellulose I to Na–cellulose IV by mercerization significantly improves the rate of enzymatic hydrolysis (Wada, Ike, & Tokuyasu, 2010). However, the stability of Na–cellulose IV, which is important for its practical applications, and the mechanism of the transition from Na–cellulose IV to cellulose II on drying are not fully understood. Therefore, in this study, we investigated the crystal structure of Na–cellulose IV using synchrotron X-ray fiber diffraction and solid-state ^{13}C NMR spectroscopy and, furthermore, the drying process from Na–cellulose IV to cellulose II was monitored using synchrotron X-ray diffraction under a controlled relative humidity (RH).

2. Experimental section

2.1. Preparation of samples

The source material used in this study was purified ramie (*Boehmeria nivea* Gaud.) fibers supplied by the Teikoku Boseki Co. (Japan). A bundle of ramie fibers (cellulose I) was aligned and fixed to a stainless steel stretching device, which was then immersed in a 3.5N NaOH solution to prepare the Na–cellulose I. The Na–cellulose IV and cellulose II samples were prepared using a repetitive alkali mercerization process with stretching of the fibers, as reported in previous publications (Hori & Wada, 2006; Langan et al., 2001). After thoroughly washing the alkali solutions with deionized water, the samples were either kept in water at room temperature or dried in air to form Na–cellulose IV or cellulose II, respectively.

2.2. Synchrotron X-ray fiber diffraction analysis

Synchrotron X-ray fiber diffraction was carried out at the BL38B1 beam line located at the SPring-8 facility (Hyogo, Japan). The oriented fibers were mounted on a goniometer head and synchrotron-radiated X-rays (λ = 1.0 Å) were irradiated for a period of 120 s orthogonal to the fiber axis. In the measurements on Na–cellulose IV, air with RH = 90% generated using a humidity generator (Shinyei SRG-1R, Japan) flowed over the sample to maintain it in the wet condition. The fiber patterns were recorded using a camera system equipped with a flat imaging plate (IP) (R-Axis V, Rigaku) at room temperature. The sample-to-IP distance was calibrated using Si powder (d = 3.1355 Å).

The peak positions of the fiber diffraction patterns were measured using the R-Axis display software package (Rigaku). After indexing the d-spacings, the unit-cell parameters were determined using a least-squares method.

2.3. Solid-state CP/MAS ^{13}C NMR spectroscopy

Solid-state ^{13}C NMR spectra were obtained using a CMX 300 spectrometer (Chemagnetics, USA) operating at 75.6 MHz. The sample was placed in a 4.0 mm zirconia rotor, and was spun at a frequency of 5 kHz in a solid-state probe at the magic angle. All spectra were obtained using a ^{1}H NMR 90° pulse length of 2.5 μs, with a cross-polarization time of 1.0 ms and a 60 kHz CW proton decoupling. The recycle time was 3 s. The spectra were calibrated using adamantane as a standard. The rotor was sealed using a Teflon cap to avoid any drying out of the Na–cellulose IV sample. Deconvolution of the spectra was carried out using a nonlinear least-square fitting procedure, where a Lorentzian function was applied to each peak.

2.4. Monitoring of the crystal transition using synchrotron X-ray diffraction

Monitoring of the drying of Na–cellulose IV was also carried out in the BL38B1 beam line at the SPring-8 facility (Hyogo, Japan), as described above. Oriented samples of Na–cellulose IV were mounted on a goniometer head in flowing humidity-controlled air from a humidity generator (Shinyei SRG-1R) at a flow rate of 1 L/min. The fiber patterns were recorded from RH = 100% to 0% in decreasing steps of 10%. The sample that had dried at RH = 0% was subsequently rewetted using a few drops of water, and the measurement was performed again at RH = 100%. Each X-ray diffraction measurement was carried out after a stabilization time of 10 min.

The equatorial and meridional X-ray diffraction profiles at each RH step were obtained by analyzing the fiber diffraction diagrams using the R-Axis display software package (Rigaku). The peak positions were determined by peak fitting the X-ray diffraction profiles, as reported previously (Wada, Okano, & Sugiyama, 1997).

3. Results and discussion

3.1. Synchrotron X-ray fiber diffraction

The synchrotron X-ray fiber diffraction diagram of the ramie fibers showed a typical pattern of cellulose I (Fig. 1a). When swollen in a 3.5N NaOH solution, the ramie fibers were converted to Na–cellulose I (Fig. 1b). Compared with cellulose I, the pattern was obscure because of the low crystallinity of Na–cellulose I and the scattering resulting from excess NaOH solution. The peak intensities were weak except for the two strong equatorial peaks occurring at 4.45 and 4.23 Å. The innermost equatorial peak occurred at 12.50 Å, which was the result of swelling of the crystalline lattice by the alkali solution.

On washing with water, all of the alkali in the crystalline lattice of Na–cellulose I was removed, causing a transition to Na–cellulose IV to occur. The X-ray diffraction pattern of a Na–cellulose IV fiber recorded at RH = 90% is shown in Fig. 1c. The d-spacings of the reflections were measured and indexed to a two-chain monoclinic unit cell (Nishimura & Sarko, 1991). The unit-cell parameters were refined as a = 9.21 Å, b = 9.87 Å, c = 10.35 Å, and monoclinic angle γ = 124.7°. The absence of any 0 0 l reflections for odd values of l indicated that the space group was $P2_1$. However, the strong reflections near the meridian on the third layer line could not be indexed to a monoclinic unit cell. Similar reflections were reported in the fiber patterns of cellulose III$_{II}$, showing that they are not true Bragg reflections but the result of diffuse scattering (Wada, Heux, Nishiyama, & Langan, 2009).

The X-ray diffraction pattern of cellulose II fibers obtained after drying Na–cellulose IV is shown in Fig. 1d. The pattern of cellulose II has sharper and more numerous peaks than the pattern of Na–cellulose IV, which means a larger crystallite size and a higher crystallinity of the cellulose II sample, but the two patterns are similar to each other (Fig. 1c and d). A major difference is the position of the innermost equatorial reflections, indexed as 1 $\bar{1}$ 0. That of cellulose II appeared at 7.29 Å versus that of Na–cellulose IV occurring at 8.42 Å. All the reflections in the pattern (Fig. 1d) were indexed using a two-chain monoclinic unit cell with a = 8.10 Å, b = 9.08 Å, c = 10.36 Å, and γ = 117.3°. From the absence of odd value 0 0 l reflections, the space group is $P2_1$. The scattering near the meridian on the third layer line, which was observed in the diagram of Na–cellulose IV, as discussed above, was also observed, but was weaker. The similarity between the patterns of Na–cellulose IV and cellulose II suggests no significant difference in the molecular conformation and packing of the cellulose

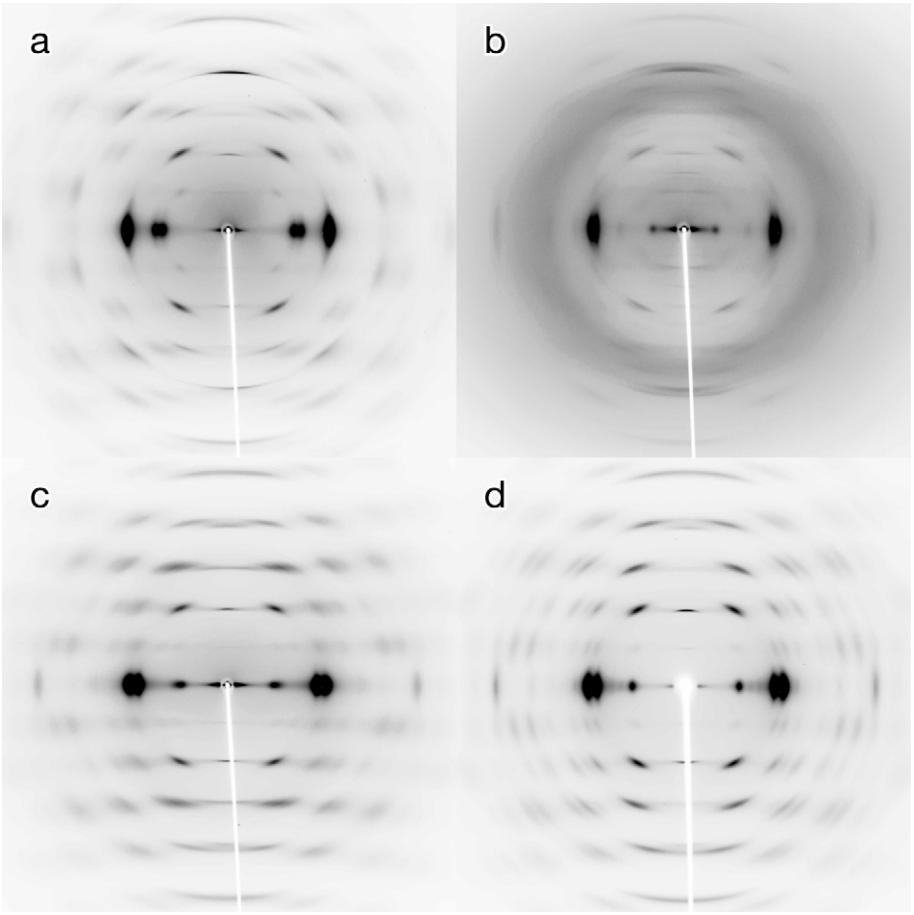

Fig. 1. Synchrotron X-ray fiber diffraction diagrams of: (a) cellulose I, (b) Na–cellulose I, (c) Na–cellulose IV, and (d) cellulose II obtained during mercerization of the ramie fibers. The diagram of Na–cellulose IV was recorded under a RH = 90% to eliminate any scattering from excess water.

in both structures. However, the unit-cell volume of Na–cellulose IV is 12% larger than that of cellulose II. The difference in volume of 12% corresponds to the volume occupied by the water molecules.

3.2. Solid-state CP/MAS ^{13}C NMR spectroscopy

Fig. 2 shows the solid-state ^{13}C NMR spectra of Na–cellulose IV and cellulose II samples. These are typical of Na–cellulose IV and cellulose II with the doublets from the C1, C4, and C6 signals (Kono, Numata, Erata, & Takai, 2004; Porro et al., 2007). Comparing both spectra, the peak positions of each carbon atom are almost the same, indicating a high degree of similarity in the molecular conformations of their cellulose chains. However, in the spectrum of Na–cellulose IV, peaks from so-called noncrystalline region occurring at 82–86 ppm and 62 ppm are larger and sharper than the peaks of cellulose II. Since Porro et al. (2007) observed similar sharp peaks in this region from a rehydrated cellulose II sample, these peaks would be ascribed to the organized molecules on the crystallite surface when the spectra were recorded in a wet condition. This result indicates small crystallite size and large surface area of Na–cellulose IV in agreement with the results of the X-ray diffraction analysis.

The C6 signals of Na–cellulose IV occurred at 63.0 and 63.6 ppm, and the C6 signals of cellulose II occurred at 63.2 and 63.9 ppm. All of these chemical shifts correspond to the *gt* conformation of the hydroxylmethyl group (Horii, Hirai, & Kitamaru, 1983). This is consistent with the X-ray structures of Na–cellulose IV and mercerized cellulose II (Langan et al., 2001; Nishimura & Sarko, 1991).

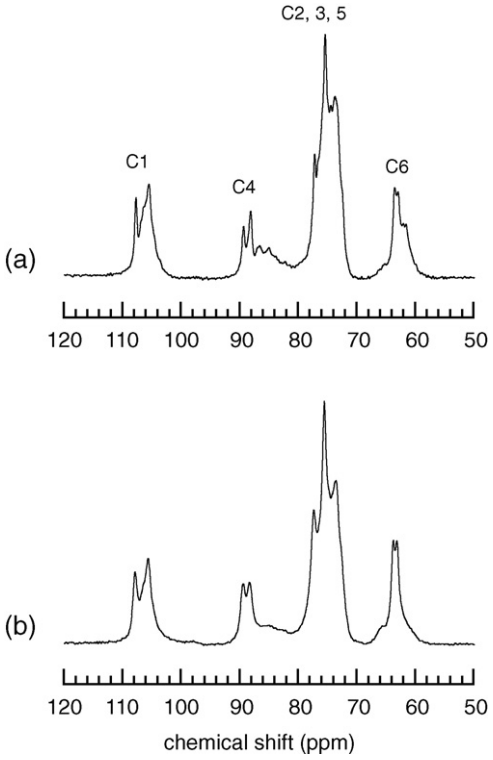

Fig. 2. Solid-state CP/MAS ^{13}C NMR spectra of: (a) Na–cellulose IV and (b) cellulose II prepared by mercerization of ramie fibers.

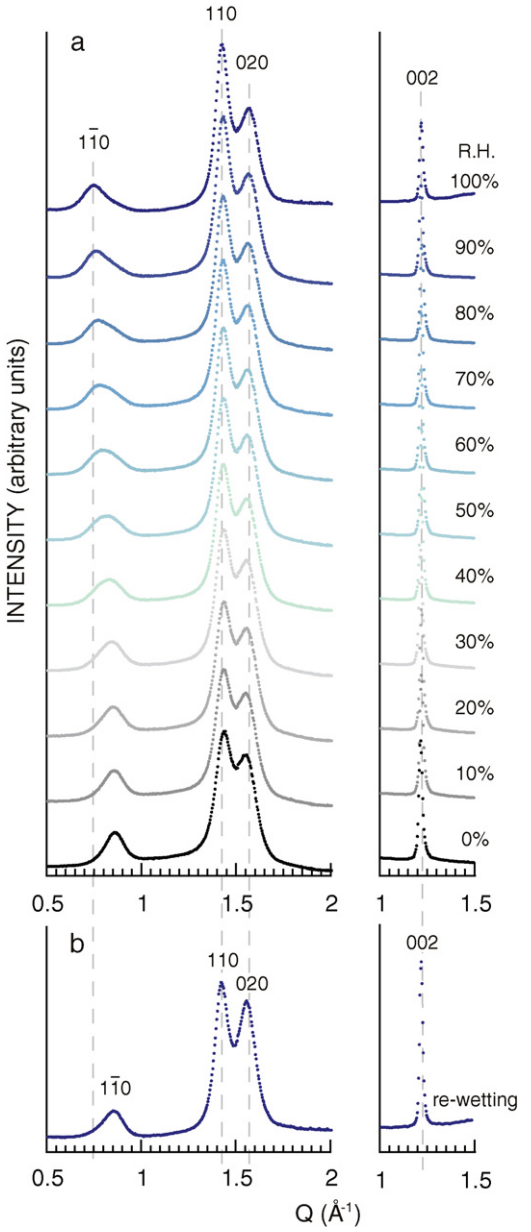

Fig. 3. Changes in the equatorial and meridional synchrotron X-ray fiber diffraction profiles: (a) during the drying of Na–cellulose IV and (b) after subsequent wetting. The term Q denotes the scattering vector ($2\pi/d$).

3.3. Crystal transition from Na–cellulose IV to cellulose II

The equatorial and meridional profiles during the drying process of Na–cellulose IV with changes in RH are shown in Fig. 3a. Three strong equatorial peaks of Na–cellulose IV and cellulose II, indexed as 1 $\bar{1}$ 0, 1 1 0, and 0 2 0, were observed for Q = 0.5–2.0 Å^{-1}, and a meridional peak, indexed as 0 0 2, was observed for Q = 1.0–1.5 Å^{-1}. At the beginning of the process (i.e., RH = 100%), the profile showed a clear pattern of Na–cellulose IV. The 1 $\bar{1}$ 0 peak, occurring at 0.74 Å^{-1} at RH = 100%, gradually shifted to higher values of Q, and broadened until RH = 50%. Subsequently, it continued to shift to higher values of Q, but gradually became sharper. Finally, the 1 $\bar{1}$ 0 peak reached Q = 0.86 Å^{-1} at RH = 0%, where the pattern only consisted of peaks from cellulose II. The other two equatorial 1 1 0 and 0 2 0 peaks remained unchanged throughout the entire process, although the peaks shifted to slightly higher and lower values of Q, respectively. The meridional 0 0 2 peak also remained at the same position, but became sharper.

The equatorial and meridional profiles of the sample that was rewetted using a few drop of water following the drying process are shown in Fig. 3b. The peak positions were almost the same as those at RH = 0%, indicating that the crystal structure was cellulose II. While the transition from Na–cellulose IV to cellulose II occurred readily on drying, the reverse transition from cellulose II to Na–cellulose IV did not occur on wetting, suggesting that the transition is irreversible. However, on wetting, slight changes in the profile were observed; in particular, the peaks became sharper except for the 1 $\bar{1}$ 0 peak. These minor changes were probably the result of the release of strain in the molecular chains induced by the adsorption of water on the crystallite surface.

The peak positions of all of the profiles recorded during the drying process shown in Fig. 3a were determined using a peak-fitting procedure, and their d-spacings were then calculated (Fig. 4). During the drying process, the d-spacing of the (1 $\bar{1}$ 0) plane, $d1\,\bar{1}\,0$,

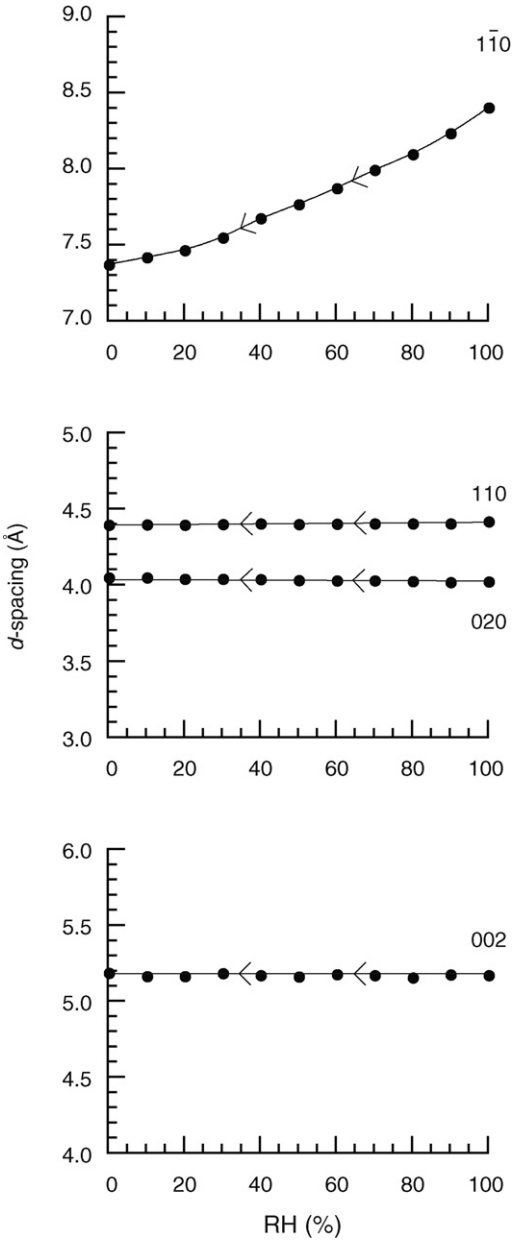

Fig. 4. Changes in the (1 $\bar{1}$ 0), (1 1 0), (0 2 0), and (0 0 2) plane d-spacing during drying of Na–cellulose IV calculated from the profiles shown in Fig. 3a.

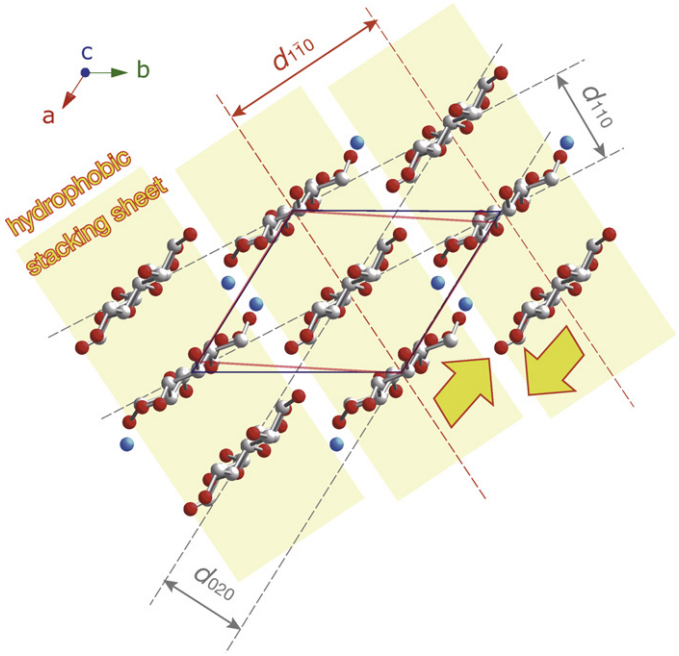

Fig. 5. Crystal structure of Na–cellulose IV viewed parallel to the *c*-axis with the contraction direction during the transition into cellulose II represented by the yellow arrows. The cellulose chains are stacked with a hydrophobic interaction along the [1 1 0] direction (hydrophobic stacking sheet), with the water molecules located between these sheets. The unit cell of cellulose II (translucent red) is superimposed on the unit cell of Na–cellulose IV (blue). When Na–cellulose IV is converted into cellulose II on dehydration, the sheets come close to each other along the *a*-axis, thus maintaining the sheet structure. (For interpretation of the references to color in this figure legend, the reader is referred to the web version of the article.)

gradually decreased from 8.45 to 7.33 Å. The other *d*-spacings, *d*110, *d*020, and *d*002, remained almost constant and stayed at approximately 4.4, 4.0, and 5.2 Å, respectively. According to the structural model of Na–cellulose IV proposed by Nishimura and Sarko (Fig. 5), the water molecules are located in the crystalline lattice between the hydrophobic stacking sheets, and the value of $d1\bar{1}0$ corresponds to the distance between these sheets. On the other hand, the values of *d*110 and *d*020 depend on the distance between the molecular chains in the sheet structure, and the value of *d*002 corresponds to half the fiber repeat distance. Thus, these results allowed us to understand the transition mechanism. Na–cellulose IV contracted while keeping its hydrophobic stacking sheet structure on dehydration, and then this was converted to cellulose II. The direction of contraction was almost parallel to the *a*-axis, based on the unit cell of cellulose II superimposed on that of Na–cellulose IV (Fig. 5).

In our previous studies on other polysaccharides, such as β-chitin and paramylon, the transition point from the hydrate to anhydrous forms was clearly observed during the drying process at RH = 30–40% for both polysaccharides (Kobayashi, Kimura, Togawa, & Wada, 2010; Kobayashi, Kimura, Togawa, Wada, & Kuga, 2010). In contrast, there is no such clear transition point in Fig. 4, where the value of $d1\bar{1}0$ decreased continuously and gradually throughout the entire drying process. This indicates that the transition from Na–cellulose IV to cellulose II did not take place at a single point, but occurred gradually with the release of water molecules from the crystalline lattice. These differences in transition behavior would be derived from the difference in the interaction between the water molecules and the molecular chains or the role of water molecules in the crystalline lattice. The water molecules in Na–cellulose IV would not have a specific interaction with the cellulose chains, and would not contribute to the stabilization of the crystal structure. Thus, the intercalating water molecules of Na–cellulose IV probably exist randomly in the crystalline lattice, and not at crystallographically defined positions to form hydrogen bonds with the cellulose chains, as in the proposed model of Na–cellulose IV (Nishimura & Sarko, 1991). This agrees with the NMR spectroscopy data, which indicated that the molecular conformation of Na–cellulose IV is similar to that of cellulose II. The unit-cell parameters of Na–cellulose IV vary among the reported studies (Nishimura & Sarko, 1991; Okano & Sarko, 1984; Sakurada & Hutino, 1936), which is probably the result of sample preparation and/or storage conditions.

Acknowledgments

The synchrotron radiation experiments were performed at BL38B1 in SPring-8 with the approval of the Japan Synchrotron Research Institute (JASRI). This work was supported in part by a grant from the Ministry of Agriculture, Forestry and Fisheries of Japan (Rural Biomass Research Project, BEC-BA252).

References

Atalla, R. H., & VanderHart, D. L. (1984). Native cellulose: A composite of two distinct crystalline forms. *Science*, *223*, 283–285.
Heines, S. V. (1944). John Mercer and mercerization, 1844. *Journal of Chemical Education*, *21*, 430–433.
Hess, K., & Trogus, C. (1931). Information about alkali cellulose. *Zeitschrift fur Phisikalische Chemie-Abteilung B-Chemie der Elementarprozesse Aufbau der Materie*, *11*, 381–408.
Hori, R., & Wada, M. (2006). The thermal expansion of cellulose II and III_{II} crystals. *Cellulose*, *13*, 281–290.
Horii, F., Hirai, A., & Kitamaru, R. (1983). Solid-state ^{13}C-nmr study of conformations of oligosaccharides and cellulose – conformation of CH_2OH group about the exo-cyclic C–C bond. *Polymer Bulletin*, *10*, 357–361.
Kamide, K., Kowsaka, K., & Okajima, K. (1985). Determination of intramolecular hydrogen bonds and selective coordination of sodium cation in alkalicellulose by CP/MASS ^{13}C NMR. *Polymer Journal*, *17*, 701–711.
Kobayashi, K., Kimura, S., Togawa, E., & Wada, M. (2010). Crystal transition between hydrate and anhydrous β-chitin monitored by synchrotron X-ray fiber diffraction. *Carbohydrate Polylmers*, *79*, 882–889.
Kobayashi, K., Kimura, S., Togawa, E., Wada, M., & Kuga, S. (2010). Crystal transition of paramylon with dehydration and hydration. *Carbohydrate Polylmers*, *80*, 492–498.
Kono, H., Numata, Y., Erata, T., & Takai, M. (2004). ^{13}C and ^{1}H resonance assignment of mercerized cellulose II by two-dimensional MAS NMR spectroscopies. *Macromolecules*, *37*, 5310–5316.
Kunze, J., Ebert, A., Schröter, B., Frigge, K., & Philipp, B. (1981). ^{13}C- ^{23}Na-NMR investigations on alkali cellulose. *Polymer Bulletin*, *5*, 399–406.
Langan, P., Nishiyama, Y., & Chanzy, H. (2001). X-ray structure of mercerized cellulose II at 1 Å resolution. *Biomacromolecules*, *2*, 410–416.
Nishimura, H., Okano, T., & Sarko, A. (1991). Mercerization of cellulose: 5. Crystal and molecular structure of Na–cellulose I. *Macromolecules*, *24*, 759–770.
Nishimura, H., & Sarko, A. (1991). Mercerization of cellulose: 6. Crystal and molecular structure of Na–cellulose IV. *Macromolecules*, *24*, 771–778.
Okano, T., & Sarko, A. (1984). Mercerization of cellulose: I. X-ray diffraction evidence for intermediate structures. *Journal of Applied Polymer Science*, *29*, 4175–4182.
Okano, T., & Sarko, A. (1985). Mercerization of cellulose: II. Alkali-cellulose intermediates and a possible mercerization mechanism. *Journal of Applied Polymer Science*, *30*, 325–332.
Philipp, B., Kunze, J., & Fink, H.-P. (1987). Solid-state carbon-13 NMR and wide-angle X-ray scattering study of cellulose disordering by alkali treatment. In R. H. Atalla (Ed.), *The structures of cellulose. Characterization of the solid states (ACS Symposium Series 340)* (pp. 178–188). Washinton, DC: American Chemical Society.
Porro, F., Bédué, O., Chanzy, H., & Heux, L. (2007). Solid-state ^{13}C NMR study of Na–cellulose complexes. *Biomacromolecules*, *8*, 2586–2593.
Sakurada, I., & Hutino, K. (1936). Über die intramizellare quellung der zellulose durch wasser. *Kolloid-Zeitschrift*, *77*, 346–351.
Sobue, H., Kiessig, H., & Hess, K. (1939). The cellulose-sodium hydroxide-water system subject to the temperature. *Zeitschrift fur Phisikalische Chemie-Abteilung B-Chemie der Elementarprozesse Aufbau der Materie*, *43*, 309–328.
Takahashi, M., Ookubo, M., & Takenaka, H. (1991). Solid state ^{13}C NMR spectra analysis of alkalicellulose. *Polymer Journal*, *23*, 1009–1014.
Takahashi, M., & Ohkubo, M. (1993). Effect of Na^+ on molecular chain of cellulose at low alkali concentration. *Journal of Japan Women's University. Faculty of Science*, *1*, 27–31.
VanderHart, D. L., & Atalla, R. H. (1984). Studies of microstructure in native celluloses using solid-state ^{13}C NMR. *Macromolecules*, *17*, 1465–1472.
Wada, M., Okano, T., & Sugiyama, J. (1997). Synchrotron-radiated X-ray and neutron diffraction study of native cellulose. *Cellulose*, *4*, 221–232.
Wada, M., Heux, L., Nishiyama, Y., & Langan, P. (2009). X-ray crystallographic, scanning microprobe X-ray diffraction, and cross-polarized/magic angle spinning ^{13}C NMR studies of the structure of cellulose III_{II}. *Biomacromolecules*, *10*, 302–309.

Wada, M., Ike, M., & Tokuyasu, K. (2010). Enzymatic hydrolysis of cellulose I is greatly accelerated via its conversion to the cellulose II hydrate form. *Polymer Degradation and Stability*, *95*, 543–548.

Warwiker, J. O. (1971). Swelling. In N. M. Bikales, & L. Segal (Eds.), *Cellulose and cellulose derivatives part IV* (pp. 325–379). New York: Wiley-Interscience.

Whitaker, P. M., Nieduszynski, I. A., & Atkins, E. D. T. (1974). Structural aspects of soda-cellulose II. *Polymer*, *15*, 125–127.

Yamada, H., Kowsaka, K., Matsui, K., Okajima, K., & Kamide, K. (1992). Nuclear magnetic study on the dissolution of natural and regenerated celluloses into aqueous alkali solution. *Cellulose Chemistry and Technology*, *26*, 141–150.

Yokota, H., Sei, T., Horii, F., & Kitamaru, R. (1990). ^{13}C CP/MAS NMR study on alkali cellulose. *Journal of Applied Polymer Science*, *41*, 783–791.